Chain structure of liquid selenium investigated by a tight-binding Monte Carlo simulation

C. Bichara and A. Pellegatti
Centre de Thermodynamique et de Microcalorimétrie du Centre National de la Recherche Scientifique, 26, rue du 141 ème R.I.A., F13003 Marseille, France

J.-P. Gaspard
Institut de Physique B5, Université de Liège, B4000 Sart Tilman, Belgium and Laboratoire pour l'Utilisation du Rayonnement Electromagnétique, Commissariat à l'Energie Atomique, Centre National de la Recherche Scientifique, et Ministère de l'Education Nationale, Bâtiment 209D, Université de Paris XI, F91405 Orsay, France
(Received 20 May 1993)

The structure of liquid and amorphous selenium has been investigated by a Monte Carlo computer simulation. The semiempirical model relies upon a tight-binding approximation of the cohesive energy. The excellent agreement of the pair correlation functions and structure factors computed at different temperatures with the experiments allows a detailed analysis of the structures. The fraction of twofold-coordinated atoms never exceeds 70%. This implies that, contrary to commonly reported ideas, the chains have to be quite short, of the order of five bonds per chain, forming a highly connected network.

I. INTRODUCTION

Se and its alloys, especially those with Te, have been extensively studied. The properties of elemental Se are intermediate between those of its chalcogen neighbors S and Te. Like sulfur, crystalline Se exhibits a large number of allotropes, all of which are twofold coordinated at normal pressures. These include trigonal Se (t-Se), the stable form at 300 K and 1.013 bar, and α, β, γ monoclinic Se. t-Se consists of parallel helical chains and the other forms are molecular crystals of Se_8 rings. As in the case of Te and most elements of groups V and VII, this low coordination number is due to a Peierls distortion. The atomic electronic structure is s^2p^4, with an s band lying well below the Fermi level (about 11 eV) and not participating in the bonding. The p-bonding mechanism tends to form a simple-cubic crystal which is unstable with respect to a Peierls distortion. As the p band is $\frac{2}{3}$ filled this leads to a structure alternating one short and two long bonds in each direction of the initial simple cubic structure.[1] Like Te, crystalline t-Se is a semiconductor under normal pressure. Under high pressure the Peierls distortion disappears causing an increase of the coordination number from 2 to 6.[2] The structure is then a rhombohedral distortion of a simple-cubic lattice and, under these conditions, Se should become metallic. Above the melting point Se remains semiconducting while Te becomes a poorly conducting metal. Liquid $Se_{1-x}Te_x$ alloys undergo a semiconductor-to-metal transition in the range $0.6<x<0.8$.[3,4] Se is able to form amorphous phases with technologically important semiconducting and photoconducting properties.[5] Among many other methods, the structure of liquid and amorphous Se has been investigated by neutron or x-ray diffraction[6,7] which gives direct information on the atomic structure. The general agreement is that liquid Se has approximately two first neighbors at a distance 2.33 Å. This coordination number, the chain structure of t-Se, and the high viscosity of Se at the melting point led to a picture of a liquid consisting of long chains, the number of atoms per chain decreasing from 10^5 to 10^6 at the melting point[8] to 7 at 1550 °C.[9] Lucovsky[10] stated that there are no Se_8 rings in the liquid state and not a majority in the amorphous state. Enderby and Barnes[11] concluded that the structural properties of liquid Se were correctly represented by a model of freely rotating chains. This picture should be confirmed by simulations that do not rely upon the assumption that chains already exist. In other words, in the spirit of the Born-Oppenheimer approximation, the buildup of a chemical bond should be the result of the position of the nuclei and of a quantum-mechanical calculation. To our knowledge, only two recent molecular-dynamics simulations of the structure exist. Balasubramanian, Damodaran, and Rao[12] performed a classical molecular-dynamics study, based on a description of the interactions with two empirical potentials: a harmonic potential describing the covalent bonding of the first-neighbor Se atoms within the chains and a Lennard-Jones potential accounting for the longer-range interactions. No angular-dependent potential was taken into account. As a result, the chain structure that was taken as an initial configuration remains without defects, and no significant four-body correlation was found. Hohl and Jones[13] used a density-functional molecular-dynamics method introduced by Car and Parrinello[14] to simulate the structure of liquid and amorphous selenium. In this method there are no approximations apart from the energy cutoff of the basis set and the description of the exchange and correlation energy. An *a priori* drawback is the small size (usually about 100 atoms) of the simulation box that can be treated. Unfortunately their results are in poor agreement with the experimental data as far as the structure factor $S(Q)$ is concerned. Nevertheless, they indicate that the atomic scale structure of liquid and amorphous selenium is more complex than a simple assembly of chains. In particular, the number of structural defects (atoms denoted Se^1 or Se^3 which depart

from the ideal coordination of 2) is found to be important. Another point is the possibility for the chains to rotate freely or not, which affects the dihedral angle distribution.

We have developed a semiempirical tight-binding (TB) Monte Carlo (MC) method which allowed us to simulate the structure of liquid arsenic and antimony[15] with a few adjustable parameters. Other authors combined the TB approximation and molecular dynamics to study small clusters of Si (Ref. 16) or liquid and amorphous Si on rather small systems of 64 atoms.[17,18] In contrast to these works, we use a moments method in the real space which avoids the full diagonalization of the Hamiltonian matrix. This enables us to treat systems as large as 648 atoms in the simulation box. A short preliminary account of this work has already been published.[19]

We first describe the method in the second section, then we present our results and compare them with the available experimental or simulation data. The results are then discussed and conclusions are drawn in the fourth section.

II. THE METHOD

The total energy used in the course of the MC simulation contains two terms: an attractive term (E_a) due to the resonance of p orbitals which is treated in the tight-binding approximation and a repulsive term (E_r) which is the sum over the relevant pairs of atoms of an empirical pairwise additive potential. The attractive energy is due to the broadening of the electronic levels into a band of partially filled states:

$$Ea=\int_{-\infty}^{E_f} En(E)dE \ , \tag{1}$$

where $n(E)$ is the electronic density of states and E_f is the Fermi level. We consider a minimal basis in the TB approximation made of p orbitals which play a dominant role in the bonding process. As the s band is nearly filled and lies well below the Fermi level, we neglect the s electrons contribution.

The $\beta_{pp\sigma}$ resonance integrals are assumed to decrease exponentially with the distance:

$$\beta_{pp\sigma}(r)=\beta^0_{pp\sigma}\exp(-qr) \ . \tag{2}$$

In a first approach we neglected the $\beta_{pp\pi}$ interactions. We shall see below that their addition does not change significantly the results. The parameters $I^0_{pp\sigma}$ and q are obtained from Robertson.[20] We took the following values:

$$\beta^0_{pp\sigma}=133 \text{ eV and } q=1.628 \text{ Å}^{-1} \ .$$

We avoid a full diagonalization of the TB Hamiltonian matrix by making use of the moments method performed at the fourth moment level.[1] In this approximation, the local density of states on each atom depends on its first- and second-neighbor positions. The integration in (1) is a three-point Gaussian integration. The empirical repulsive potential (E_r) is parametrized as

$$E_r=V_0(r_0/r)^p \ , \tag{3}$$

where r_0 is the distance unit in our calculations. It is taken as the edge of a hypothetical undistorted simple-cubic structure at the same density (ρ) as crystalline t-Se:

$$r_0=\rho^{-1/3}=3.0 \text{ Å} \ .$$

V_0 is calculated assuming that the minimum of the total energy, which has a simple pairwise form in this limiting case, is then located in $r=r_0$:

$$V_0=\frac{2\beta^0_{pp\sigma}qr_0\exp(-qr_0)}{\sqrt{3}p} \ . \tag{4}$$

The remaining free parameter p is adjusted in order to fit the first peak position of the experimental pair correlation function $g(r)$. In this simple approach, the relative hardness of the repulsive potential p/qr_0 is the key quantity that indicates whether or not the Peierls distortion survives in the liquid state.[15] At given density and temperature, a low value of p/qr_0 (i.e., a soft repulsive potential) favors the Peierls distortion, whereas a high value of p/qr_0 (i.e., a hard repulsive potential) indicates that the Peierls distortion has disappeared. In the present instance p is equal to 5 ($p/qr_0=1.02$), indicating that the system is highly distorted (for stability reasons, p has to be larger than qr_0), in agreement with the simple picture of a liquid with two short and strong covalent bonds per atom.

The Monte Carlo simulations were done under canonical conditions (648 atoms in a box of $24.7\times28.5\times32.4$ Å^3), 2000 MC steps per atom were performed, and the averages were taken over 50 independent configurations. The cutoff distance for the energy calculation was taken at 3.70 Å. The density ($\rho=0.0284$ atom/Å^3) is the experimental one. The temperature ($kT=0.08$ eV) was adjusted so as to fit the experimental $g(r)$ and $S(Q)$ of Ref. 7 at 531 K. With such a crude model for the total energy of the system, a better agreement between the temperature of the simulation and the experimental one would be fortuitous. Moreover, we compare a simulated $g(r)$ calculated directly on the atomic positions with the experimental one which has been damped by the transfer function of the experimental apparatus. This is probably a reason why the temperature of the simulation is higher than the experimental one.

III. RESULTS

A. Pair correlation function, structure factor, and coordination number

Figure 1 shows the pair correlation function $g(r)$ compared to the experimental one at 531 K.[6,7] Except for the small third peak at 5.9 Å which will be discussed later, and the peak heights, the agreement is excellent. It is a general feature of all the simulations, in which the correlation function is directly measured on the atomic positions, to yield peak heights larger than the experimental ones. In the latter case, the peaks are smoothed by the transfer function of the experimental spectrometer. The agreement is even better as far as the structure factor is concerned, as shown in Fig. 2. The peculiar shape of this

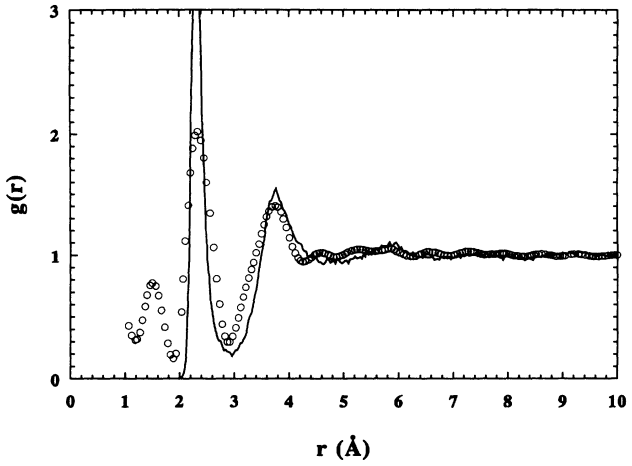

FIG. 1. Pair correlation function of liquid Se: circles, experiment (Ref. 7) at 531 K; solid line, simulation with 648 atoms.

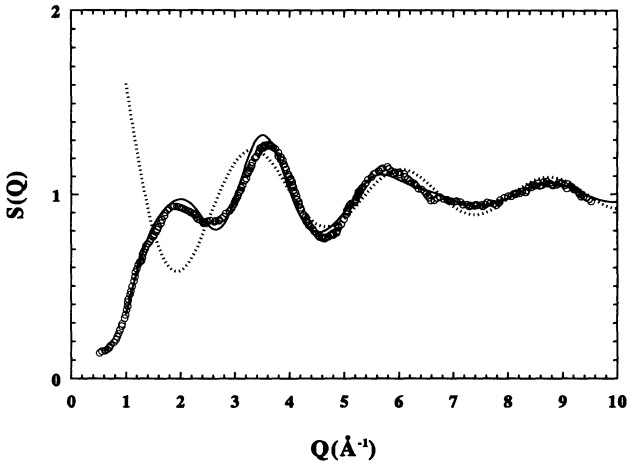

FIG. 3. Structure factor of liquid Se: circles, experiment (Ref. 7) at 531 K; solid line, simulation with 64 atoms; dotted line, Fourier transform of a Dirac δ function at $r_1=2.33$ Å (see text).

structure factor, exhibiting a first peak at $Q=1.87$ Å^{-1}, with a height lower than one, is interesting to consider. Except for the first one, all the peaks are in phase with the Fourier transform of a single Dirac δ function at $r_1=2.33$ Å (the position of the first-neighbor peak) which writes

$$S_1(Q)=1+4\pi\rho r_1 \sin(Qr_1)/Q \ . \tag{5}$$

This is shown in Fig. 3 and means that the correlations beyond the first-neighbor position affect mostly the first peak in $S(Q)$. To this regard, the results of Hohl and Jones[13] are rather unsatisfactory, as the first peak of their simulated $S(Q)$ lies at 2.55 Å^{-1} instead of 1.87 Å^{-1}. The size of the simulation box is not responsible for this discrepancy as we were able to obtain a structure factor of the same quality by performing a simulation with our previous input parameters in a box containing 64 atoms (see Fig. 3). The main difference between Hohl and Jones' results and ours lies in the region between the first and second peak of $g(r)$: the gap between them is much deeper in our results and in the experiment. The larger dispersion of the first-neighbor distances could be the cause of the discrepancy. However, in agreement with these authors, we find a distribution of first neighbors with significant Se^1 and Se^3 contributions, as can be seen in Table I. The average number of first neighbors is found to be 2.1 by integrating the radial distribution function $G(r)=4\pi\rho r^2 g(r)$ from $r=0$ to the first minimum at 2.92 Å. This distance will be used throughout the paper to define the first neighbors in the analysis of the structure. The distribution of neighbors shown in Table I is not very sensitive to the choice of this cutoff distance in the sense that the fraction of twofold-coordinated atoms remains constant around 70% whatever the cutoff distance between 2.70 and 3.10 Å.

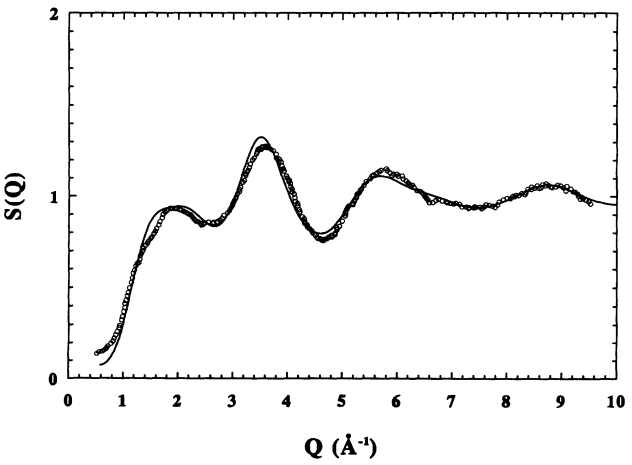

FIG. 2. Structure factor of liquid Se: circles, experiment (Ref. 7) at 531 K; solid line, simulation with 648 atoms.

B. Higher-order correlations

The bond angle distribution $B(\theta)$ depicted in Fig. 4 exhibits a rather narrow distribution centered around 106°, a slightly higher value than that of t-Se (103°). This is consistent with the value that can be deduced from the

TABLE I. Distribution of atomic coordination in liquid Se.

Number of neighbors	Frequency (%)	Average distance (Å)
1	11	2.30
2	71	2.36
3	18	2.50

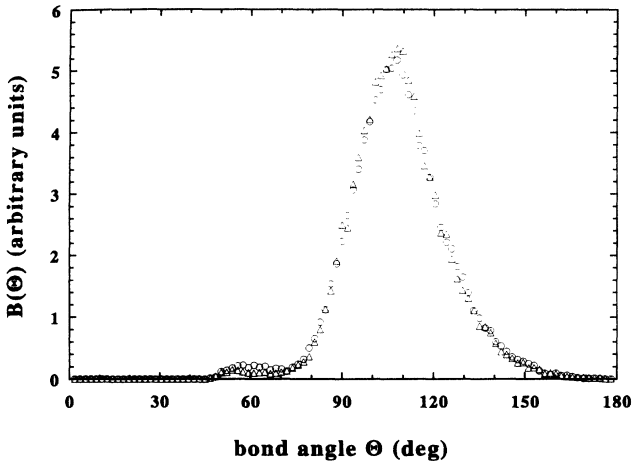

FIG. 4. Bond angle distribution in liquid Se: circles, simulation with 648 atoms; triangles, simulation with 64 atoms.

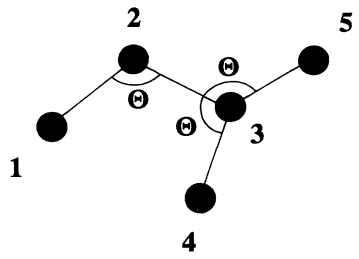

FIG. 6. A possible local atomic configuration in liquid Se: all bond distances are 2.33 Å, the bond angles Θ are 106°, $d_{13}=3.75$ Å and $d_{14}=3.64$ Å contribute to the second peak of $g(r)$.

positions of the first two peaks in $g(r)$ (106°) and with the other simulation results. The dihedral angle distribution $D(\phi)$ (Fig. 5) is nearly flat, exhibiting a smooth maximum around 0°, which means that four atoms have a slight preference to remain in the same plane, like atoms 1, 2, 3, and 4 in Fig. 6. As the distances 1–3 and 1–4 contribute to the second peak in $g(r)$, this is consistent with the experimental data. The small hump of the simulated $g(r)$ at $r=5.9$ Å has been shown in Ref. 6 to be consistent with a random distribution in $D(\phi)$. The absence of structure in $D(\phi)$ shows that neither an energy preference nor a steric effect favor a given dihedral angle. In particular, there is no preference for a dihedral angle $\phi=102°$, the characteristic value of the t-Se helices. We conclude that the structure of liquid Se does not contain helical chains.

C. Analysis of the structure in terms of rings and chains

As the calculated $g(r)$ and $S(Q)$ fit rather well the experimental data it is worth analyzing the details of the atomic structure. In particular, we calculated the number and the length of the chains that can be found in the structure by linking together atoms separated by less than 2.92 Å. The chain length is defined as the number of bonds linking a series of twofold-coordinated Se^2 atoms and the end of chains which are either Se^1 or Se^3 atoms. As can be seen from Fig. 7, there is about six times more chains than rings in the structure. Both chains and rings are rather short: an average value of 4.2 bonds was found for the chains and 4.9 bonds for the rings. The Se_8 rings encountered in the crystalline α and β phases are totally absent in the liquid structure. Only 4% of the chains have free ends of Se^1 atoms, 32% of them are of the type Se^1-$(Se^2)_n$-Se^3, and the rest are of the type Se^3-$(Se^2)_n$-Se^3. These statistics shows that the structure of liquid Se consists of highly connected short chains.

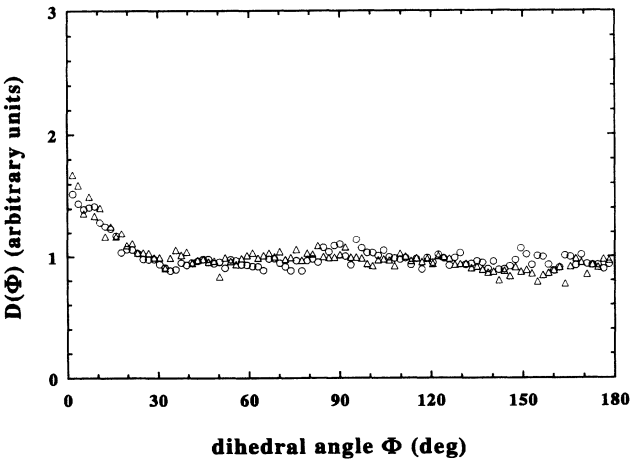

FIG. 5. Dihedral angle distribution in liquid Se: circles, simulation with 648 atoms; triangles, simulation with 64 atoms.

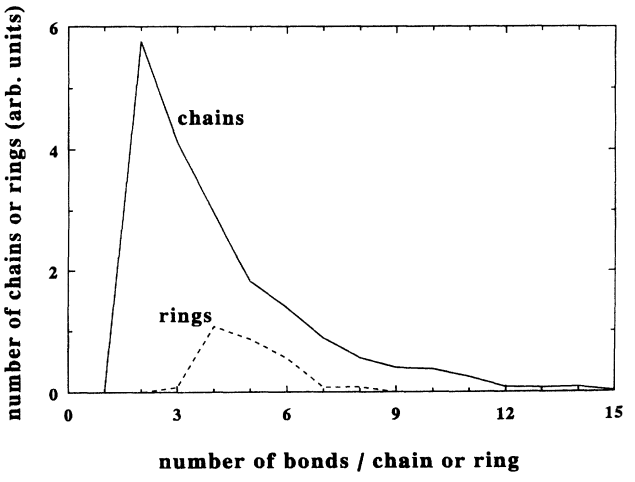

FIG. 7. Distribution of chain and ring lengths in liquid Se.

D. Influence of the $\beta_{pp\pi}$ interactions

The $\beta_{pp\pi}$ interactions that have been so far neglected for the sake of simplicity can be included and the resonance integrals are parametrized in the same way as the $\beta_{pp\sigma}$:

$$\beta_{pp\pi}(r)=\beta^0_{pp\pi}\exp(-qr)\ . \tag{6}$$

This simply adds one electronic structure parameter that can be taken from Robertson[20] and consequently the value of our empirical repulsive energy parameter has to be modified in order to maintain the correct first peak position. With $\beta^0_{pp\pi}=-35$ eV we had to take $p=5.7$ to obtain the same agreement for $g(r)$ and $S(Q)$. No major changes were observed, even in the dihedral angles distribution. As most of the paths on this structure are self-retracing at the fourth moment level, we cannot expect any torsional rigidity.

E. Amorphous selenium

Starting from a configuration of Se in the liquid state at $kT=0.10$ eV an amorphous state has been obtained by quenching to a temperature of $kT=0.02$ eV. The parameters of the calculation were the same as the previous ones in the liquid ($\beta^0_{pp\sigma}=133$ eV, $q=1.628$ Å^{-1}, $p=5$), except for the density that was the experimental one in the amorphous state ($\rho=0.0326$ atom/Å^3). The calculated structure factor is compared with the experimental one[6,7] in Fig. 8. The agreement is not as good as for the liquid. Although $S(Q)$ correctly reproduces characteristic features of the amorphous state (e.g., the small peak around 6.8 Å^{-1}), its second and third peaks are slightly shifted towards lower Q values. Nevertheless, it has to be emphasized that the adjustable parameter p has not been changed to improve the agreement. The structure has been analyzed in the same way as above and no major change was observed: the distributions are narrower but no striking new feature appears.

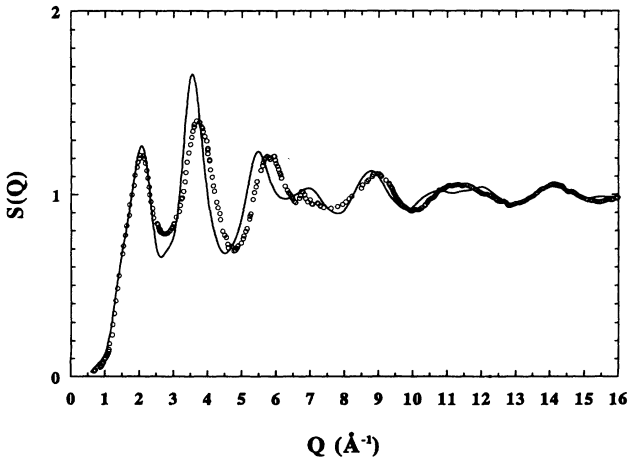

FIG. 8. Structure factor of amorphous Se: circles, experiment (Ref. 7); solid line, simulation with 648 atoms.

IV. DISCUSSION AND CONCLUSION

In this study, our attempts have been twofold. We first have tried to apply a semiempirical model, already used in the case of the group-V elements (As and Sb) (Ref. 15) for the total energy of liquid selenium. The tight-binding approximation combined with the moments method performed at the fourth moment's level is relevant from the point of view of the quantum mechanics that govern such a system with covalent bonds and a Peierls distortion. Second, we have attempted to reproduce, as close as possible, the pair correlation function and the structure factor in order to analyze the atomic scale structure. A simple view of one of the configurations that have been generated (Fig. 9) can summarize our findings: in this model, liquid Se consists of rather short branched chains. The bond length and bond angles of crystalline Se remain, but the dihedral angle distribution is nearly random. This disorder creates a large number of defects that drastically reduce the chains length, making of liquid Se a kind of branched polymer. In agreement with the Car-Parrinello simulations of Hohl and Jones,[13] we found that only 70% of the atoms are twofold coordinated. This implies that the chains have to be rather short (about five bonds per chain) in order to accommodate the 30% defects. We conclude that, despite an average coordination number of 2.1, liquid selenium is not made of long chains. This result has to be related to our previous study of liquid arsenic[15] for which, despite its coordination number just above 3 as in the crystalline state, the liquid structure is not made of disordered corrugated planes but is a more complicated structure with two-, three-, and fourfold coordinated atoms. Although the pair correlation func-

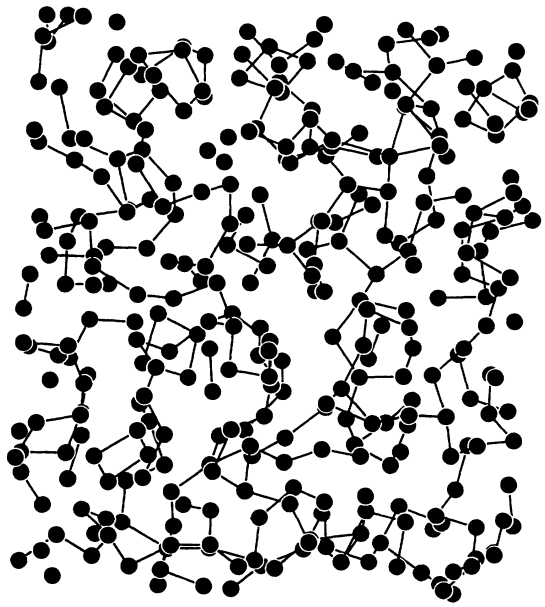

FIG. 9. A configuration of liquid Se. The neighbors at distances less than 2.92 Å are linked together. A small slice has been cut in the box to preserve the legibility.

tions and structure factors of liquid and amorphous Se can also be represented by models of "nearly free rotating chains,"[6] we believe that such purely topological models that do not treat properly the process of chemical bonding are not reliable to give an insight into the atomic scale structure. Nevertheless, both approaches suffer from the fact that they rely only upon a comparison with the experimental pair correlation functions and structure factors. To this regard our simulations are not conclusive as they yield neither dynamical properties nor the electronic density of states to compare with other experimental data. It should be of interest to measure the proportion of dangling bonds (or Se^1 atoms) in amorphous Se to check the validity of our main result that was also found in Ref. 13, namely, the presence of a large number of "defects" in the structure.

ACKNOWLEDGMENTS

Financial support from Belgium FRFC (Contract No. 2.4515.90) and Belgium-France exchange program agreements (Contract No. 93-57) are gratefully acknowledged.

[1]J.-P. Gaspard, F. Marinelli, and A. Pellegatti, Europhys. Lett. **3**, 1095 (1987).
[2]T. Krüger and W. B. Holzapfel, Phys. Rev. Lett. **69**, 305 (1992).
[3]L. A. Silva and M. Cutler, Phys. Rev. B **42**, 7103 (1990).
[4]J. R. Magana and J. S. Lannin, Phys. Rev. B **29**, 5663 (1984).
[5]*The Physics of Selenium and Tellurium,* Proceedings of the Internationl Conference on the Physics of Selenium and Tellurium, Königstein, FRG, 1979, edited by E. Gerlach and P. Grosse (Springer, Berlin, 1979).
[6]R. Bellissent, Nucl. Instrum. Methods **199**, 289 (1982).
[7]T. Bellissent and G. Tourand, J. Non-Cryst. Solids **35&36**, 1221 (1980).
[8]R. C. Keezer and M. V. Bailey, Mater. Res. Bull **2**, 185 (1967).
[9]W. W. Warren and R. Dupree, Phys. Rev. B **22**, 2257 (1980).
[10]G. Lucovsky, *The Physics of Selenium and Tellurium* (Ref. 5), pp. 178–192.
[11]J. E. Enderby and A. C. Barnes, Rep. Prog. Phys. **53**, 85 (1990).
[12]S. Balasubramanian, K. V. Damodaran, and K. J. Rao, Chem. Phys. **166**, 131 (1992).
[13]D. L. Hohl and R. Jones, Phys. Rev. B **42**, 3856 (1991).
[14]R. Car and M. Parrinello, Phys. Rev. Lett. **55**, 2471 (1985).
[15]C. Bichara, A. Pellegatti, and J.-P. Gaspard, Phys. Rev. B **47**, 5002 (1993).
[16]K. Laasonen and R. M. Nieminen, J. Phys. C **2**, 1509 (1990).
[17]L. Goodwin, A. J. Skinner, and D. G. Pettifor, Europhys. Lett. **9**, 701 (1989).
[18]C. Z. Wang, C. T. Chan, and K. M. Ho, Phys. Rev. B **39**, 8586 (1989).
[19]C. Bichara, A. Pellegatti, and J.-P. Gaspard, Proceedings of the 8th International Conference on Liquid and Amorphous Metals (LAM8), Vienna, 1992 [J. Non-Cryst. Solids **156-158**, 68 (1993)].
[20]J. Robertson, Adv. Phys. **32**, 361 (1983).